Digital Communications and Networks 7 (2021) 1–15

Contents lists available at ScienceDirect

Digital Communications and Networks

journal homepage: www.keaipublishing.com/dcan

Directional neighbor discovery in mmWave wireless networks

Yu Wang [a], Ticao Zhang [a], Shiwen Mao [a,*], Theodore (Ted) S. Rappaport [b]

[a] Department of Electrical and Computer Engineering, Auburn University, Auburn, AL, 36849-5201, USA
[b] NYU WIRELESS Center, NYU Tandon School of Engineering, Brooklyn, NY, 11201, USA

ARTICLE INFO

Keywords:
Fifth generation (5G) wireless
Beamforming
Spatial filtering
Directional antenna
Directional neighbor discovery
Initial access
Millimeter wave (mmWave) networks
Spatial rendezvous

ABSTRACT

The directional neighbor discovery problem, i.e., *spatial rendezvous*, is a fundamental problem in millimeter wave (mmWave) wireless networks, where directional transmissions are used to overcome the high attenuation. The challenge is how to let the transmitter and the receiver beams meet in space under *deafness* caused by directional transmission and reception, where no control channel, prior information, and coordination are available. In this paper, we present a *Hunting-based Directional Neighbor Discovery* (HDND) scheme for ad hoc mmWave networks, where a node follows a unique sequence to determine its transmission or reception mode, and continuously rotates its directional beam to scan the neighborhood for other mmWave nodes. Through a rigorous analysis, we derive the conditions for ensured neighbor discovery, as well as a bound for the worst-case discovery time and the impact of sidelobes. We validate the analysis with extensive simulations and demonstrate the superior performance of the proposed scheme over several baseline schemes.

1. Introduction

The drastically increasing wireless data has triggered huge interest in 5G wireless systems, in which the millimeter wave (mmWave) communication has been recognized as a key component because the huge amount of spectrums in the mmWave bands can enable multi-Gigabit wireless networks and support bandwidth-intensive applications [1–4]. However, many challenges need to be addressed in order to fully harvest the high potential of mmWave communications. Specifically, mmWave signals experience considerably higher attenuation than lower frequencies [5]. Furthermore, such signals usually do not easily penetrate or diffract around obstacles [3]. Consequently, smart antennas and beamforming are indispensable for combating the high attenuation and achieving high data rates [6,7,17]. As a result, although having been studied in the context of cellular and ad hoc networks, there has been renewed interest in the design of directional networks [8–11]. A particular fundamental problem in such networks is how to discover neighbors under *deafness* caused by directional transmission and reception, along with other relevant problems, including the need to bootstrap directional beam steering in a mmWave network without prior information and coordination, and to maintain network connectivity when nodes come and go and as propagation conditions and topology vary over time. Fast algorithms that do not require centralized control and coordinated operations, yet with guaranteed performance, would be highly appealing.

Neighbor discovery is a fundamental component for distributed, autonomous wireless networks [26]. The use of directional antennas has merits, but also causes many challenges. Many existing neighbor discovery schemes assume certain channel models. The mmWave channel is sparse due to the limited number of dominant propagation paths [5,24,36]. In Ref. [17], compressed sensing based low-complexity algorithms are proposed to exploit channel sparsity for adaptively estimating multipath mmWave channel parameters. In Ref. [18], a method is proposed for estimating the receive-side spatial covariance matrix of a channel from a sequence of power measurements made at random angles.

Directional neighbor discovery is actually a *spatial rendezvous problem*, where the directional beams of a pair of nodes need to meet in space (i.e., pointing to each other or both viewing a strong reflector), with one node in the transmission mode and the other in the receiving mode. Existing neighbor discovery schemes for directional wireless networks exploit several approaches to overcome the deafness problem, e.g., (i) adopting the omni-directional transmission/reception [10–14], (ii) using the synchronized operation [12,13,15], (iii) utilizing a common control channel [15], and (iv) transmitting at random directions and exploiting reflected signals [16–19]. In the context of cellular mmWave networks, the directional neighbor discovery is also called as the *initial access*

* Corresponding author.
E-mail addresses: yzw0049@auburn.edu (Y. Wang), tzz0031@auburn.edu (T. Zhang), smao@ieee.org (S. Mao), tsr@nyu.edu (T.(T.S. Rappaport).

https://doi.org/10.1016/j.dcan.2020.09.005
Received 7 July 2020; Accepted 15 September 2020
Available online 28 September 2020

problem, i.e., the procedure with which a mobile device establishes an initial link layer connection to a base station [19–22]. For example, the authors in Ref. [19] proposed a directional cell discovery procedure, where base stations periodically transmit synchronization signals at random directions, and mobile devices scan for such signals to detect a base station. In Ref. [23], a deterministic approach is proposed with bounded discovery time in a sector-based directional network by applying the Chinese Remainder Theorem [25].

1.1. Related work

Existing directional neighbor discovery algorithms can be roughly classified as follows:

Algorithms using other spectrum bands. In Ref. [15], the authors present a multi-band directional neighbor discovery scheme, where a common control channel on the 2.4 GHz WiFi band is assumed to identify potential neighbors. This is a centralized algorithm for neighbor discovery for the 60 GHz WiFi. Using the 2.4 GHz WiFi channel is helpful, since all the nodes are within one-hop range in the 2.4 GHz WiFi band, although they may not be one-hop neighbors in the 60 GHz WiFi band.

Algorithms using omni-directional communications. In Ref. [13], a synchronized, slotted time scheme is proposed, which utilizes a directional antenna at the transmitter to enhance the gain, and an omni-directional antenna at the receiver to increase the reception probability. This approach is also used in Ref. [31] for neighbor discovery in the 60 GHz Wireless Personal Area Networks (WPAN), where an Angle-of-Arrival (AOA) based algorithm is developed to locate the transmitter. In Ref. [12], a synchronized, slotted time algorithm is presented, which incorporates an antenna without beamforming (*N*–BF), Transmitter Beamforming only (T-BF), and Transmitter and Receiver Beamforming (TR-BF) at different stages of neighbor discovery with a purely randomized scheme. In Ref. [32], the authors present the Talk More Listen Less (TMLL) design principle to reduce idle-listening in neighbor discovery, which is more suitable for wireless sensor networks, where energy consumption is a major concern and transmissions are broadcast-based. In these works, omni-directional communications help to mitigate the deafness problem.

Algorithms with Synchronized Operation. Many schemes require synchronized, slotted time operation [12,13,15,31]. Some other schemes make stronger assumptions on synchronized operation [33,34], e.g., (i) all transmitters face a certain direction, (ii) all receivers face the opposite direction simultaneously, and (iii) all nodes sweep at the same angular speed. Such strongly synchronized operations may lead to more collisions. In Ref. [33], a three-way handshake and a random response scheme are proposed to reduce the collision probability. In Ref. [34], a token-based algorithm is developed to ensure that only one node transmits beacon signals at a time.

Randomized Asynchronous Algorithms. Randomized, asynchronous schemes have been developed in Refs. [13,18,19,35]. It has been shown that asynchronous algorithms require at least twice as much time than a synchronized algorithm for a *K*-clique network [13]. Moreover, the performance of an asynchronous algorithm is usually worse than that of a synchronized algorithm in general one-way handshake networks [35].

Deterministic Algorithms. In Ref. [34], the neighbor discovery process is sequentially conducted by the nodes (i.e., as a serialized process), and the scheme discovers all sector-to-sector links between nodes with a systematic approach. In Ref. [23], all pairs of sectors of the directional antennas are examined under the guidance of the Chinese Remainder Theorem. The proposed oblivious neighbor discovery protocol is proved to achieve guaranteed neighbor discovery with the bounded time under the assumption of ideal beacons (i.e., it takes zero time to transmit and receive).

1.2. Contributions and organization

In this paper, we consider an mmWave ad hoc network deployed in a 2D area and develop an effective scheme for neighboring nodes (or, users) to discover each other. Since neighbor discovery is the first step to start a self-configuring wireless network, it may not be easy to acquire prior information for centralized coordination, synchronization, or acquiring a common control channel. On the other hand, letting the receiver work in the omnidirectional mode (at a lower rate) can help to mitigate the blindness problem. However, the omnidirectional receiver may receive beacons from multiple neighbors simultaneously and thus at smaller SNR per received signal, leading to interference (i.e., more collisions) and requiring more processing to decode the different beacon signals in a dense network. Unlike prior approaches, here we develop an effective directional neighbor discovery scheme without using omnidirectional transmissions, without needing a common control channel, and without needing time synchronization and synchronized operation, yet with guaranteed neighbor discovery performance. In other words, we are interested in "blind" neighbor discovery with only directional antennas (also termed "oblivious neighbor discovery" in Ref. [23]). As shown below, this approach offers promise for mobile or fixed mmWave networks that seek to maximize SNR through narrow-beam antenna implementation whenever possible.

In our proposed scheme, a node continuously rotates its directional beam in the either clockwise or counterclockwise direction to scan its neighborhood to discover neighbors in a quasi-static mmWave network. While this work is focused on 2D, it should be clear that the method described here could be extended to 3D neighbor discovery by incorporating a suitable 3D channel model [24], for use in networks involving users that have a wide variation in relative elevation, such as drones, or for mobile networks for users in high rise buildings. With the proposed scheme, each node operates in either the *transmission mode* or the *reception mode*. In the transmission mode, the node sends out a beacon signal, stops and starts to listen for acknowledgments (ACK) from neighbors. The node in the transmission mode repeats the beacon-listen pattern to sweep the neighborhood. In the reception mode, the node keeps listening for beacon signals. If a beacon sign is received, it responds with an ACK immediately on the same channel to the direction where the beacon signal was received. Once a beacon-ACK handshake is completed, the two nodes find each other.

We call this approach *Hunting-based Directional Neighbor Discovery* (HDND) since each node continuously scans its neighborhood to "hunt" for neighbors during the neighbor discovery period. Considering a pair of neighboring nodes, the node with a faster angular velocity for rotating its antenna beam will chase and catch up with the antenna beam of the slower node in a finite time. Following the notation in Ref. [26], this is a "deterministic" approach, as opposed to random (or, probabilistic) schemes that point to random directions to find neighbors.

Specifically, with the proposed scheme, each node generates its *pseudo-slot sequence* consisting of its ID in the binary form: a sequence of 0 bits and a sequence of 1 bits. Each bit in the pseudo-slot sequence corresponds to a pseudo-slot of time. In each pseudo-slot, each node determines its state by the corresponding sequence bit value: transmission mode if the bit is a 0 and reception mode if the bit is a 1. A transmitter scans its neighborhood by rotating its beam with angle velocity ω_T. During the scanning process, the transmitter sends a beacon signal and then starts to listen for ACKs. It repeats the beacon-listen operation until an ACK is received (i.e., a neighbor is discovered). A receiver also rotates its beam with angle velocity ω_R while continuously listening for beacons. If a beacon is received, the receiver will reply immediately with an ACK. If the ACK is successfully received by the transmitter node, a successful handshake is completed, and the pair of nodes discover each other.

In this paper, we first consider the basic case of a single pair of nodes, one is in the transmission mode and the other is in the reception mode. We derive the condition for the transmitter and receiver beams to meet in the 2*D* space, the distribution of the overlap angle of the two beams, as well as the condition for a successful beacon-ACK handshake (which indicates a successful neighbor discovery). The analysis also sheds useful

insights on how to set the protocol parameters to ensure a successful neighbor discovery. We then study the case of a distributed ad hoc network in which the nodes are randomly placed in either transmission or reception modes. We adopt the special sequence design presented in prior work [23,27] to coordinate the transmission/reception mode of each node without centralized control. We show that when combined with the basic case design of a single transmitter-receiver pair, the proposed scheme can ensure neighbor discovery in a bounded time. We derive the process of ensured discovery, as well as the bound of the worst-case discovery time, and validate our analysis with extensive simulations. We also provide an analysis of the impact of sidelobes on the neighbor discovery performance. Compared with two baseline schemes, the proposed algorithm can achieve a considerable reduction in neighbor discovery time as well as improved network throughput.

The remainder of this paper is organized as follows. Section 2 presents the system model and assumptions. Section 3 discusses the basic case of a transmitter-receiver pair. The proposed scheme for a distributed mmWave ad hoc network is presented in Section 4. We will then analyze the impact of sidelobes on the neighbor discovery performance in Section 5. Section 6 presents our performance research. Section 7 concludes this paper and discusses the future work.

2. System model and assumptions

We consider an ad hoc mmWave-based network, in which a set of nodes are deployed randomly in a region. We first present the system model and our basic assumptions below.

Unique ID: Each node is assigned a unique ID before it joins the network. Note there is no need to know other nodes' IDs for neighbor discovery.

Steerable Smart Antenna: Each node is equipped with a smart antenna [6], which can continuously steer its beam towards a desired direction [7,17].

Beamwidth: The beamwidth of a transmitter, denoted as θ_T, and that of a receiver, denoted as θ_R, are constants during the neighbor discovery process, with $0 < \theta_T < 2\pi$ and $0 < \theta_R < 2\pi$.

Antenna Pattern: The antenna pattern for all transceivers is directional (i.e., directional transmitters and directional receivers). The quasi-omnidirectional pattern is not considered since it is inefficient from a link SNR perspective, and not suitable for reliable mmWave networks [2,29]. The pattern of a directional antenna usually consists of one main lobe and several sidelobes. To simplify the model, we first ignore the sidelobes and assume that the antenna has an ideal gain, as in the previous works [30].[1] We will then consider the case of sidelobes in Section 5. Let φ be the pointing angle, which may be within the range of deviation from the center (i.e., the boresight) of the beam. The antenna gain can be modeled as

$$g(\varphi) = \begin{cases} G(\theta), & |\varphi| < \theta/2 \\ 0, & \text{otherwise}, \end{cases} \tag{1}$$

where $G(\theta)$is the antenna gain as a function of the antenna beamwidth θ.

Communication Modes: We assume the general case of half-duplex communications. Once turned on, each node operates in one of two modes, i.e., the *transmission mode* or the *reception mode*. In the transmission mode, a node first sends a short discovery beacon signal and then listens for a short period of time for ACK from a discovered neighbor (if any). It rotates its beam and repeats the beacon-listening operation while scanning its adjacent areas. In the reception mode, the node continuously listens to the channel while rotating its beam. If a beacon signal is received, it will immediately return an ACK message in the direction of receiving the beacon signal. If the overlapping part of the two beams is sufficiently wide, then the ACK will be received, and a successful neighbor discovery is achieved. An example of the communication modes is given in Fig. 1.

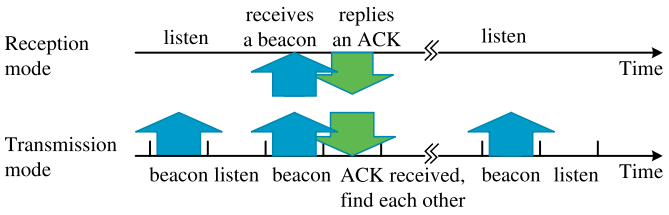

Fig. 1. Example of the transmission and reception modes. The time slot in the figure has a duration of a beacon signal duration τ_B (plus certain guard time for propagation delay). The first beacon signal is not received since the two beams are not pointing to each other. The second beacon signal is received, and the receiver responds with an ACK message, which completes the neighbor discovery procedure.

Steering Model: Each node can continuously rotate its beam at a constant angular velocity ω_T in the transmission mode and at a different constant angular velocity ω_R in the reception mode, under constraint that $\omega_T \neq \omega_R$.[2] The same beamwidth, i.e., θ_T and θ_R, and the same antenna gain, i.e., $G(\theta_T)$ and $G(\theta_R)$, are maintained for all the transmitters and receivers, respectively. The angular velocities should satisfy the following constraint:

$$\frac{\omega_R}{\omega_T} = \frac{p}{q}, \ \mathbf{s.t.}\ p, q \in \mathbb{Z}^+, \ p \neq q, \ \text{and} \ \ \gcd(p, q) = 1, \tag{2}$$

where p and q are different, co-prime, positive integers, and $\gcd(\cdot,\cdot)$ returns the greatest common divisor. If the condition is not satisfied, e.g., $\omega_R = \omega_T$, the two nodes may never find each other.

Discovery Beacon Signal: Each node in the transmission mode continuously sends discovery beacon signals, which carries the transmitter's Unique ID. The transmission time of a discovery beacon signal, termed as the *beacon duration*, is a short, constant duration denoted by τ_B. Without losing generality, we assume that the ACK message has a similar format to the beacon signal, which carries the Unique ID of the node in the reception mode, and the transmission time for an ACK is also τ_B.

Successful Neighbor Discovery A successful neighbor discovery for a pair of nodes *i* and *j* is achieved if node *i* receives the ID of node *j* in a beacon signal, and then node *i* responds with an ACK message that carries its ID and is received by node *j*, or vice versa.

3. Neighbor discovery for a single transmitter-receiver pair

For the sake of explanation, we first study the basic situation of a pair of mmWave nodes, one operating in the transmission mode and the other in the reception mode. The findings in this section will then be leveraged to address the case of an mmWave ad hoc network in Section 4.

3.1. Conditions for space rendezvous

With the model described in Section 2, a simple approach is to have the transmitter and receiver point their beams in random directions. They will discover each other if their beams happen to meet in space (i.e., spatial rendezvous with partial overlap of the pair of beams). However, such a random approach usually leads to a non-negligible probability of missed detection [16]. To mitigate the worst-case performance of

[1] Sidelobes may be helpful to neighbor discovery, but may also cause more collisions of beacons and ACKs. Attenuated sidelobes will generally be weaker than the main beam. The receiver can keep track of relative signal levels to determine the best beam.

[2] All the nodes in the transmission mode use the same $\omega_T$and all the nodes in the reception mode use the same ω_R. This is pre-configured in the protocol implementation, and of course could be varied as a function of application or node or channel variations.

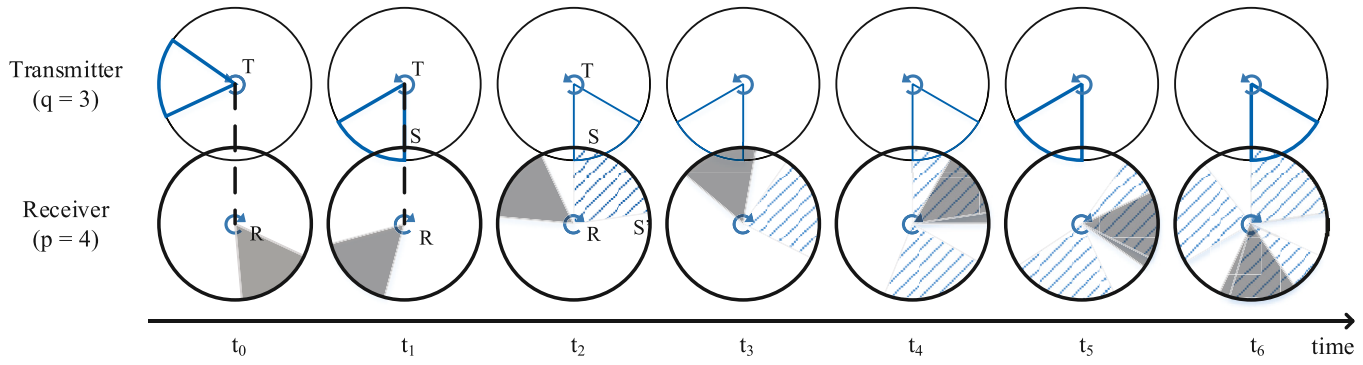

Fig. 2. Relative beam directions of the transmitter and receiver during the neighbor discovery process, in which each beam rotates in a given direction (i.e., clockwise or counterclockwise) at a constant angular velocity (i.e., ω_T or ω_R). The beam positions of the transmitter and receiver at specific time instances (e.g., $t_0, t_1, \ldots$) are illustrated as a blank sector and a gray-colored sector, respectively. Note that the time instances are not necessarily evenly spaced. For example, from t_1 to t_2, the transmitter rotates 60° in the counterclockwise direction, while the receiver rotates 80° in the clockwise direction; from t_2 to t_3, the transmitter rotates 300° in the counterclockwise direction while the receiver rotates 400° in the clockwise direction. The ratio is $\omega_T/\omega_r = 60/80 = 300/400 = 3/4$.

probabilistic approaches, a *deterministic* algorithm is considered in this paper.

As described in Section 2, each node randomly picks a direction (i.e., clockwise or counterclockwise) to rotate its beam at a fixed angular velocity (i.e., ω_T or ω_R, respectively). During the rotation process, the node in the transmission mode repeats the operations of sending a beacon signal and then listens for ACKs, while the node in the reception mode continuously listens for beacon signals until they meet in space and complete a beacon-ACK handshake. We have the following theorem for the two beams to meet in space.

Theorem 1. *Consider the transmitter-receiver pair case: the receiver has beamwidth θ_R and angular speed ω_R, and the transmitter has beamwidth θ_T and angular velocity ω_T. The angular velocities satisfy constraint (2). The receiver is guaranteed to receive a beacon signal from the transmitter within p rounds (when the transmitter will rotate for q rounds), if and only if the following constraint is satisfied, regardless of the starting positions and rotating directions of the two beams.*

$$p\theta_T + q\theta_R > 2\pi. \tag{3}$$

Proof. Let us begin with a simple example of $p = 4$, $q = 3$, and $\theta_T = \theta_R = \pi/3$. It can be verified that conditions (2) and (3) are satisfied. Without losing generality, the receiver (R) rotates clockwisely and the transmitter (T) rotates counterclockwisely, as shown in Fig. 2. Let t_i's be the specific time instances during the scanning process. The initial positions of the transmitter/receiver beams at t_0 are shown in Fig. 2. The transmitter beam is marked as a solid-lined sector, and the receiver beam is marked in a shade of gray.

The two nodes can communicate with each other when their beams meet in space, more specifically, when the transmitter's signal travels along the line connecting them, TR (i.e., *Line of Centers* (LoC)), and the reception beam covers the LoC at the same time, as the case at time t_3 in Fig. 2.

In Fig. 2, snapshots of the transmitter/receiver antenna beams at different time instances are shown to explain the "hunting" process. Specifically, t_1 and t_2 are the time instances that the transmitter beam starts to reach and leave the LoC during the first round of rotation, respectively. From time t_1 to time t_2, the receiver radius RS rotates to a new position RS'. The area it sweeps through during this period is marked as a *striped sector* at time t_2 in Fig. 2. After the transmitter beam rotates for $q = 3$ rounds, and while the receiver beam rotates for $p = 4$ rounds, there will be three such striped sectors, as shown at time t_6 in Fig. 2.

The striped sectors are generated when the transmitter beam sweeps through the LoC. It can be seen that $t_2 - t_1 = \theta_T/\omega_T$ and thus the central angle of a striped sector is $\omega_R \cdot \theta_T/\omega_T = \theta_T \cdot p/q = 4\pi/9$. Therefore, after the transmitter beam rotates for $q = 3$ rounds, there will be 3 such striped sectors, each with central angle $4\pi/9$. Since the transmitter beam rotates at a constant speed, the striped sectors are evenly distributed in the receiver disk, separated by 3 *blank sectors*, each with central angle $2\pi/9$ (see time t_6 in Fig. 2).

This simple example can be easily generalized. In the general case, after the transmitter beam rotates for exactly q rounds, there will be q striped sectors and zero or q blank sectors. Each time the transmitter beam sweeps through the LoC, the duration is θ_T/ω_T and the central angle of each striped sector is $\omega_R \cdot \theta_T/\omega_T = \theta_T \cdot p/q$. The central angle for each blank sector is $(2\pi - p\theta_T)/q$ when $p\theta_T < 2\pi$; otherwise, If $p\theta_T \geq 2\pi$, the entire receiver disk will be covered in stripes.

Therefore, it can be guaranteed that the receiver will receive part of the beacon after rotating for p rounds if and only if the receiver beam (the

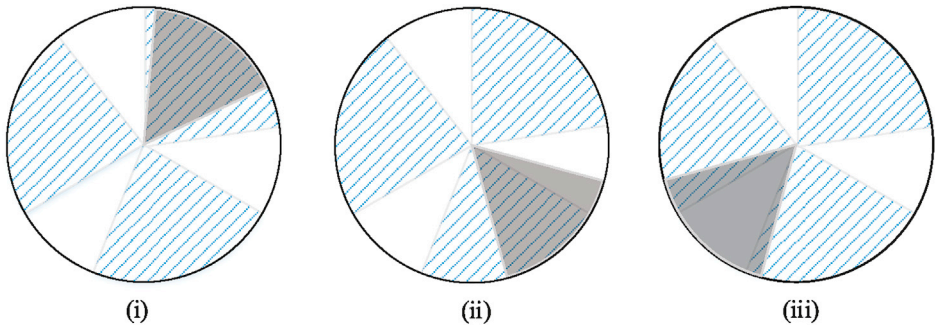

Fig. 3. Three cases for the receiver beam to overlap with the striped sectors. This is the result for the example shown in Fig. 2, after the transmitter beam rotates for $q = 3$ rounds.

gray-colored sector) overlaps with any striped sectors. When there are blank sectors, this situation means the central angle of a blank sector should be smaller than that of the receiver beam (i.e., the receiver beam is not completely covered in a blank sector area). This fact translates to the following condition:

$$\frac{2\pi - p\theta_T}{q} < \theta_R \;\Rightarrow\; p\theta_T + q\theta_R > 2\pi. \tag{4}$$

when there are no blank sectors (i.e., when $p\theta_T \geq 2\pi$), the receiver beam will fall completely within the striped area (i.e., the entire disk). We have $p\theta_T + q\theta_R > p\theta_T \geq 2\pi$. Combining these two conditions, we have (3).

3.2. Conditions for a successful discovery

Theorem 1 provides the condition that the transmitter and receiver beams meet in space. However, for a successful neighbor discovery, the overlapping angle of the two beams should be sufficiently large for the beacon-ACK handshake to complete. Define Θ_m as the maximum angle of the overlap of the transmitter and receiver beams. In this section, we provide an analysis of Θ_m to derive its distribution. The analysis also provides the condition for a successful neighbor discovery.

Without losing generality, we assume $p\theta_T > q\theta_R$ in this section (the analysis for the case of $p\theta_T < q\theta_R$ is similar). As shown in the example in Fig. 2, the positions of the striped areas at time t_6 depends only on the initial position of the transmitter beam. Then, as shown in Fig. 3, if the condition in Theorem 1 is met, there are three possible cases for the transmitter and receiver beams to meet in space:

1. The receiver beam is fully covered in a striped sector (as in Fig. 3(i)), due to the assumption $\theta_R < \theta_T \cdot p/q$;
2. The receiver beam partially overlaps with *one* striped sector (as in Fig. 3(ii));
3. The receiver beam partially overlaps with *two* striped sectors (as in Fig. 3(iii)), since $\theta_R > (2\pi - p\theta_T)/q$(see Theorem 1).

In Case 1, we have $\Theta_m = \theta_R$ and this happens with the probability $(p\theta_T/q - \theta_R)/(2\pi/q) = (p\theta_T - q\theta_R)/(2\pi)$.

In Case 2, part of the receiver beam is covered by a striped area and the other part is covered by a blank area with a central angle of $(2\pi - p\theta_T)/q$. We have $\Theta_m \tilde{} U[(p\theta_T + q\theta_R - 2\pi)/q, \theta_R]$, i.e., Θ_m is uniformly distributed. This happens with the probability $2 - p\theta_T/\pi$.

In Case 3, the receiver beam overlaps with two striped sectors; the blank area between the two striped areas is completely covered by the receiver beam. We pick the larger one of the two overlapping areas for Θ_m, which is also uniformly distributed as $U[(p\theta_T + q\theta_R - 2\pi)/(2q), (p\theta_T + q\theta_R - 2\pi)/q]$. This case happens with the probability $(p\theta_T + q\theta_R)/(2\pi) - 1$.

Therefore, Θ_m has the following distribution.

$$\Theta_m \tilde{} \begin{cases} \theta_R, & \text{w.p. } \dfrac{p\theta_T - q\theta_R}{2\pi} \\ U\left[\dfrac{p\theta_T + q\theta_R - 2\pi}{q}, \theta_R\right], & \text{w.p. } 2 - \dfrac{p\theta_T}{\pi} \\ U\left[\dfrac{p\theta_T + q\theta_R - 2\pi}{2q}, \dfrac{p\theta_T + q\theta_R - 2\pi}{q}\right], & \text{w.p. } \dfrac{p\theta_T + q\theta_R}{2\pi} - 1. \end{cases}$$

The Probability Density Function (PDF) of Θ_m is

$$f(\theta_m) = \begin{cases} \dfrac{p\theta_T - q\theta_R}{2\pi} \cdot \delta(\theta_m - \theta_R), \text{if } \theta_m = \theta_R \\ \dfrac{q}{\pi}, \text{if } \dfrac{p\theta_T + q\theta_R - 2\pi}{q} < \theta_m < \theta_R \\ \dfrac{q}{\pi}, \text{if } \dfrac{p\theta_T + q\theta_R - 2\pi}{2q} \leq \theta_m \leq \dfrac{p\theta_T + q\theta_R - 2\pi}{q}. \end{cases}$$

$$= \begin{cases} \dfrac{p\theta_T - q\theta_R}{2\pi} \cdot \delta(\theta_m - \theta_R), \text{if } \theta_m = \theta_R \\ \dfrac{q}{\pi}, \text{if } \dfrac{p\theta_T + q\theta_R - 2\pi}{2q} \leq \theta_m < \theta_R, \end{cases} \tag{5}$$

where θ_m is the value that r.v. Θ_m takes, and $\delta(\cdot)$ is the Dirac delta function. The complementary cumulative density function (Complementary CDF) of Θ_m is

$$\overline{F}(\theta_m) = \begin{cases} 0, & \text{if } \theta_m > \theta_R \\ \dfrac{p\theta_T + q\theta_R - 2q\theta_m}{2\pi}, & \text{if } \dfrac{p\theta_T + q\theta_R - 2\pi}{2q} \leq \theta_m \leq \theta_R \\ 1, & \text{if } \theta_m < \dfrac{p\theta_T + q\theta_R - 2\pi}{2q}. \end{cases}$$

Define $\tau = 2\tau_B$ as the *handshake time*, i.e., the minimum time required for a successful beacon-ACK handshake. Also let D denote a successful neighbor discovery event. Let r.v. $\mathscr{T}$ denote the duration when the two beams overlap, and the probability for a successful handshake can be derived as

$$P_\tau(D|\mathscr{T} = t) = \begin{cases} 0, & t \leq \tau \\ t/\tau - 1, & \tau < t < 2\tau \\ 1, & t \geq 2\tau. \end{cases} \tag{6}$$

We define threshold $\theta_{th} = \tau\omega_R = 2\tau_B\omega_R$, then the successful handshake probability can be written as

$$P_{\theta_{th}}(D|\Theta_m = \theta_m) = \begin{cases} 0, & \theta_m \leq \theta_{th} \\ \theta_m/\theta_{th} - 1, & \theta_{th} < \theta_m < 2\theta_{th} \\ 1, & \theta_m \geq 2\theta_{th}. \end{cases} \tag{7}$$

Theorem 2. *Consider the transmitter-receiver pair case. Assuming $p\theta_T + q\theta_R > 2\pi$ and $p\theta_T > q\theta_R$, then for $\theta_{th} = \tau\omega_R$, the probability for a successful handshake after the transmitter beam rotates for q rounds has the following distribution.*

$$P_{\theta_{th}}(D) = \begin{cases} 0, \text{ if } \theta_{th} > \theta_R \\ \dfrac{q\theta_{th}^2 - q\theta_R\theta_{th} + p\theta_T\theta_R - p\theta_T\theta_{th}}{2\pi\theta_{th}}, \\ \text{if } \dfrac{\theta_R}{2} < \theta_{th} \leq \theta_R \\ \dfrac{p\theta_T + q\theta_R - 3q\theta_{th}}{2\pi}, \\ \text{if } \dfrac{p\theta_T + q\theta_R - 2\pi}{2q} < \theta_{th} \leq \dfrac{\theta_R}{2} \\ \dfrac{p\theta_T + q\theta_R - \pi - 2q\theta_{th}}{2\pi} - \dfrac{(p\theta_T + q\theta_R - 2\pi)^2}{8q\theta_{th}\pi}, \\ \text{if } \dfrac{p\theta_T + q\theta_R - 2\pi}{4q} < \theta_{th} \leq \dfrac{p\theta_T + q\theta_R - 2\pi}{2q} \\ 1, \text{ if } \theta_{th} \leq \dfrac{p\theta_T + q\theta_R - 2\pi}{4q}. \end{cases} \tag{8}$$

Proof. From (7), we have the probability of a successful handshake conditioned on Θ_m. Combining with the distribution of Θ_m given in (5), the probability of having a successful handshake can be derived as

$$P_{\theta_{th}}(D) = \int_0^\infty P_{\theta_{th}}(D|\Theta_m = \theta_m) f(\theta_m) d\theta_m = \int_{\frac{p\theta_T + q\theta_R - 2\pi}{2q}}^{\theta_R} P_{\theta_{th}}(D|\Theta_m = \theta_m) \frac{q}{\pi} d\theta_m + \frac{1}{2\pi}(p\theta_T - q\theta_R) P_{\theta_{th}}(D|\theta_R). \tag{9}$$

The second term in (9) is the integral of the Delta function in (5).

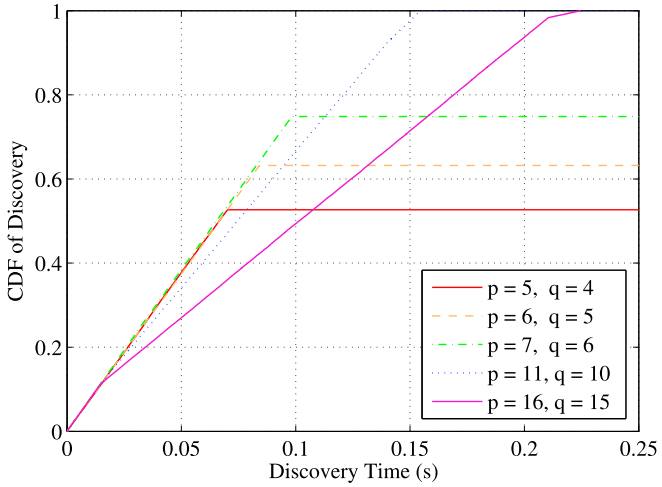

Fig. 4. Cumulative discovery probability versus different p and q values.

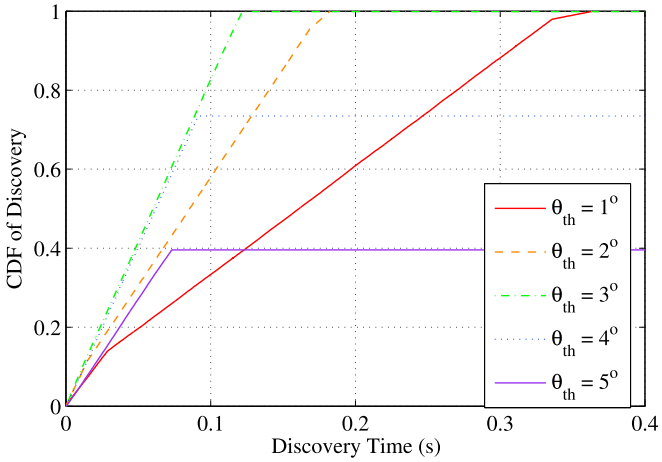

Fig. 5. Cumulative discovery probability versus different θ_{th} values.

Substituting (7) into (9), then we have (8).

Theorem 2 indicates that the following corollary holds true, which follows directly from (8).

Corollary 2.1. *If the chosen parameters satisfy*

$$\frac{p\theta_T + q\theta_R - 2\pi}{4q\omega_R} > \tau, \tag{10}$$

a successful discovery will be guaranteed within q rounds of the transmitter beam rotation.

Corollary 2.2. *A successful discovery will be guaranteed within a time interval of $2\pi/\omega_0$, where $\omega_0 = \omega_T/q = \omega_R/p$.*

Proof. Following Corollary 2.1, the neighbor discovery will be guaranteed within q rounds of transmitter's rotation while each round takes time $2\pi/\omega_T$. Thus, the total time for q rounds is $\frac{2\pi}{\omega_T} \times q = \frac{2\pi}{\omega_0}$

If the equality in (10) holds, then we have $\omega_0 = (p\theta_T + q\theta_R - 2\pi)/(4qp\tau)$. For fixed θ_R, θ_T, and τ, we have $\frac{\partial\omega_0}{\partial q} = \frac{2\pi - p\theta_T}{4pq^2\tau}$. As the proof of Theorem 1 shows, if $p\theta_T \geq 2\pi$, the entire receiver disk will be covered in stripes. This is a an ordinary case that neighbor discovery will always be successful. If $p\theta_T < 2\pi$, this is the more critical case shown in Fig. 3. Then, we have $\frac{\partial\omega_0}{\partial q} > 0$, i.e., ω_0 increases with q. This can be also shown for p due to the symmetry of p and q. According to Corollary 2.2, the neighbor discover time decreases with p and q. Therefore, it is desirable to choose smaller values of p and q while satisfying the conditions in Theorem 1 and Corollary 2.1.

Table 1
Simulation parameters.

Parameter	Value
Network area	20 m × 20 m
Transmission range	2.5/5.0/7.5/10.0/12.5 m
Number of nodes	10, 20, 30, 40
Directional beamwidth	30°
Control package length	1074 bytes
Data package length	10 Mbytes
Control data rate (mmWave band)	27.5 Mbps
Data transmission rate	2503 Mbps

3.3. Simulation validation

In Figs. 4 and 5, we give simulation results of the transmitter-receiver pair case to validate Theorems 1 and 2. We set both θ_T and θ_R to 30°. Both beacon signals and ACK messages are 1074 bits, and the control channel data rate is 27.5 Mbps (as in Table 1). We then examine the impact of the rotation parameters p and q, and the threshold θ_{th}. The results are obtained from 100,000 simulations with different random seeds.

We find that the simulation results closely match the analysis summarized in the two theorems. Therefore, we omit the analysis curves in both figures for clarity. In Fig. 4, we plot the CDF of neighbor discovery assuming $\theta_{th} = 2°$ to validate Theorem 1. It can be seen that if p and q are small, there is no guarantee of successful discovery over a certain amount of time since Condition (3) is not satisfied (e.g., when $p = 5$ and $q = 4$, and when $p = 6$ and $q = 5$, the curves do not hit 100%). When $p = 7$ and $q = 6$, although Condition (3) is satisfied, the overlap of the two beams (i.e., Θ_m) is still too small to guarantee a successful handshake. When p and q are sufficiently large, the CDF curves will reach 100%, as in the cases when $p = 11$ and $q = 10$, and when $p = 16$ and $q = 15$. Also, it can be seen that for $p = 11, q = 10$ and $p = 16, q = 15$, the neighbor can be discovered with the probability 1, while the worst case neighbor discovery time is 0.153s and 0.223s, respectively.

In Fig. 5, we set $p = 8$ and $q = 7$, which satisfies (3). According to Theorem 2, if θ_{th} is larger than $(p\theta_T + q\theta_R - 2\pi)/(4q)$(which is 3.2143° in this case), the maximum probability of discovery should be smaller than 1. That is, the successful neighbor discovery may not be guaranteed. For example, we may see the cases when $\theta_{th} = 4°$ and when $\theta_{th} = 5°$ in Fig. 5, where neighbor discovery may not be guaranteed since the condition in Theorem 2 is violated. In conclusion, the system parameters θ_R, θ_T, p, q, ω_R, and ω_T must be carefully chosen according to Theorems 1 and 2 to guarantee 100% neighbor discovery performance.

4. Hunting-based directional neighbor discovery

Now, we consider the neighbor discovery problem in a distributed ad hoc mmWave network with multiple nodes. The key is to make one of the two autonomous neighbors operate in the transmission mode, and the other in the reception mode. We show that this can be achieved with a specific sequence as presented in previous works [23,27]. Another issue

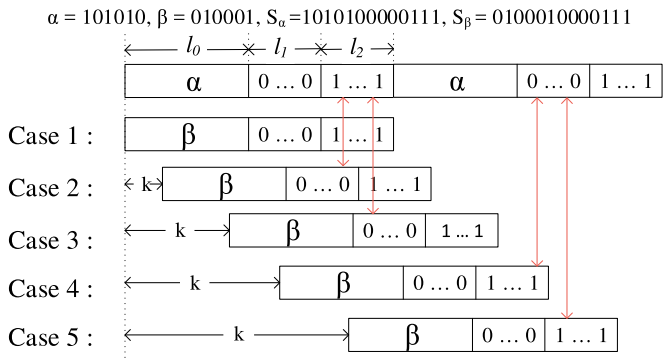

Fig. 6. Example of sequences for mode matching: $\alpha = 101010$, $\beta = 010001$, $l_1 = 4$, and $l_2 = 3$.

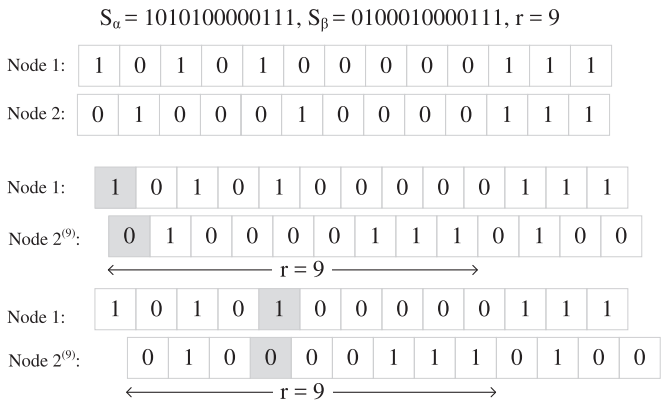

Fig. 7. Find two pseudo-slots with different bits when the pseudo-slots of the two nodes are not exactly aligned (the cyclic rotation delay of node 2's sequence is 9, denoted as Node $2^{(9)}$).

is the asynchronized operations of the nodes. Additional discovery time is required when the operations are not synchronized. We then derive the worst-case bound for neighbor discovery time and present the general neighbor discovery algorithm.

4.1. Mode matching

Define a *pseudo-slot* as an interval with duration $2\pi q/\omega_T$ (or, $2\pi p/\omega_R$, which is the same due to (2)). That is, the transmitter beam can rotate q rounds, and the receiver beam can rotate p rounds during a pseudo-slot. If a pseudo-slot is marked with a "1," the corresponding node operates in the *transmission mode*; if the pseudo-slot is marked with a "0," the corresponding node operates in the *reception mode* (see the definitions of the transmission and reception modes in Section 2). Then, we can assign a sequence of 0's and 1's to each node to control the node's operation mode during the neighbor discovery process without a centralized control. If we can guarantee that one node's "1" pseudo-slot meets the other node's "0" pseudo-slot at least once before the sequence runs out, then these two nodes are guaranteed to find each other if the parameters are set according to Theorem 2.

In Refs.[23, 27], a specific control sequence is used to ensure that pseudo-slots of different states meet in time for two neighboring nodes. The sequence consists of the node's unique ID, followed by an l_1-bit segment of 0's and an l_2-bit segment of 1's. As in the example in Fig. 6, node 1 has ID $\alpha = 101010$ with the length $l_0 = 6$, and node 2 has ID $\beta = 010001$ with the same length. Then, the sequences for the two nodes are 1010100000111 and 0100010000111, respectively. The length of both sequences is $L = l_0 + l_1 + l_2 = 6 + 4 + 3 = 13$. In Refs. [23,27], the authors prove that such two sequences can guarantee that the two nodes can operate in different modes in at least one-bit duration under all possible cyclic rotations within L continuous positions.

Consider different ways of relative cyclic rotations in general while the pseudo-slots of the two nodes are aligned. Using the node 1 sequence as a reference, the node 2 sequence can have a cyclic rotation delay k, and $k \in [0, L-1]$. As illustrated in Fig. 6, there are five cases for the relative cyclic rotation delay k.

- Case 1: $k = 0$. The two sequences are exactly aligned (i.e., α is exactly aligned with β). Since both α and β are unique IDs, there will be at least one-bit location in the first l_0-bit segment that the two sequences have difference values.
- Case 2: $k \in [1, l_2]$. The last bit of the 0-segment in the node 2 sequence is aligned with a bit in the 1-segment in the node 1 sequence. So at least at this bit position, the node 1 bit is "1" and the node 2 bit is "0."
- Case 3: $k \in [l_2 + 1, l_1 + l_2 - 1]$. The first bit of the 0-segment in the node 2 sequence is aligned with a bit in the 1-segment of the node 1 sequence. So at least at this bit position, the node 1 bit is "1" and the node 2 bit is "0."
- Case 4: $k \in [l_0 + 1, l + l_1 - 1]$. The last bit of the 1-segment in the node 2 sequence is aligned with a bit in the 0-segment in the node 1 sequence. So at least at this bit position, the node 1 bit is "0" and the node 2 bit is "1."
- Case 5: $k \in [l_0 + l_1, l + l_1 + l_2 - 1]$. The first bit of the 1-segment in the node 2 sequence is aligned with a bit in the 0-segment in the node 1 sequence. So at least at this bit position, the node 1 bit is "0" and the node 2 bit is "1."

Therefore, the following fact is ensured according to Refs. [23,27].

Fact 1. *Using the two sequences, each consists of the node's unique ID, an l_1-bit segment of all 0's and an l_2-bit segment of 1's guarantee that there is at least one pseudo-slot within which the two nodes are in different operation modes during a total period of L pseudo-slots, under the condition that $l_1 + l_2 \geq l_0$* [23,27].

We next consider the more general scenario where the pseudo-slots of the two nodes are not aligned (i.e., no time and slot synchronization). Let the relative cyclic rotation of node 2 sequence be between r and $r+1$, i.e., r slots plus a random *drift*, which is shorter than a pseudo-slot. Then, each pseudo-slot of node 1 will overlap at least half of that of node 2. For example, in Fig. 7, the relative cyclic rotation of the node 2 sequence is 9 pseudo-slots (denoted as Node $2^{(9)}$). If the drift is less than 0.5 pseudo-slot, the node 1 sequence has a different bit value from that of node $2^{(9)}$ at the first slot, which is greater than half pseudo-slot long. Otherwise, the node 1 sequence has a bit value different from that of node $2^{(9)}$ at the fifth slot, which is more than half of the pseudo slot length. Thus, we redefine the duration of the pseudo-slot (given at the beginning of Section 4.1) as the time of $2q$ rounds of the transmission mode (which is also the time of $2p$ rounds of the reception mode), i.e., $4\pi q/\omega_T$ (or $4\pi p/\omega_R$). Using the new definition, the above design can ensure successful neighbor discovery, even if the pseudo-slots of the two nodes are not aligned.

4.2. Neighbor discovery algorithm

Recall that a successful neighbor discovery requires that

1. one node receives the other node's ID in a beacon signal, and
2. the node returns its ID in an ACK that is successfully received by the beacon node.

In Section 4.1, the adopted sequences ensure that within L pseudo-slots, there will be at least one pseudo-slot, with one node in the transmission mode and the other in the reception mode. The transmitter will repeat the process of sending a beacon signal and listening for ACK. The receiver will keep listening for beacon signals and reply with an ACK immediately when a beacon signal is received. In this way, neighbor discovery can be ensured, as summarized in the following theorem.

Theorem 3. *If two nodes follow the distributed neighbor discovery procedure given below, then a successful neighbor discovery is guaranteed for the node pair within L pseudo-slots.*

1. *Each node generates a pseudo-slot sequence consisting of its unique ID (length l_0), a segment of $\left\lfloor \frac{l_0}{2}+1 \right\rfloor$ 0's, and a segment of $\left\lceil \frac{l_0}{2} \right\rceil$ 1's.*
2. *In any pseudo-slot with the duration $4\pi q/\omega_T$ (or $4\pi p/\omega_R$), if the bit in the sequence is 1, the node repeats the process of sending a beacon signal (for τ_B seconds) and waiting for ACK (for another τ_B seconds), and scans its neighborhood for 2q rounds. If the bit in the sequence is 0, the nodes keeps listening for beacon signals, while scanning its neighborhood for 2p rounds. If a beacon signal is received, the node will decode the beacon signal to obtain the transmitter's ID, and then immediately return an ACK that carries its own ID.*
3. *Each beacon signal lasts for $\tau_B = (p\theta_T + q\theta_R - 2\pi)/(8q\omega_R)$.*

Proof. From part 1) of Theorem 3, we have $\left\lfloor \frac{l_0}{2} \right\rfloor + 1 + \left\lceil \frac{l_0}{2} \right\rceil \geq l_0 + 1 > l_0$. Then, following Fact 1 in Section 4.1, the two nodes are guaranteed to meet in time with different modes for at least half of a pseudo-slot (when there is no synchronization) within a period of $L = 2l_0 + 1$ pseudo-slots.

From part 2) of Theorem 3, a half pseudo-slot time is sufficient for the transmitter beam to rotate for q rounds and for the receiver beam to rotate for p rounds.

From part 3) of Theorem 3, we have $2\omega_R\tau_B = (p\theta_T + q\theta_R - 2\pi)/(4q)$. Following Theorem 2, a discovery is ensured within q rounds of transmitter beam rotation.

The detailed neighbor discovery algorithm is presented in Algorithm 1. Line 1 in Algorithm 1 generates a pseudo-slot sequence to determine the operation mode of the node. Line 4 reads the mode of the current pseudo-slot from the sequence. If it is 1, the node will operate as a transmitter, and execute Lines 5–12 to hunt for a neighbor that is in the reception mode. Otherwise, the node operates as a receiver and executes Lines 14–20. It keeps listening for beacon signals. When a beacon signal is received, it returns an ACK to the sender to the direction where the beacon signal comes (see Fig. 1). Note that the algorithm is not terminated after discovering a neighbor. Rather, the algorithm will continue to find other neighbors, if any. According to Theorem 3, any pair of nodes should complete neighbor discovery within L pseudo-slots. The algorithm is terminated after L pseudo-slots when all the potential neighbors are found.

Algorithm 1. Hunting-based directional neighbor discovery algorithm

```
1  Each node generates its pseudo-slot sequence S
   consisting of its ID (l_0 bits), ⌊l_0/2⌋ + 1 "0" bits, and ⌈l_0/2⌉
   "1" bits;
2  i ← 0;
3  if i < L then
4      if S(i) = 1 then
5          Continuously sends a beacon signal and listens
           for ACK alternatively for 2q rounds with angle
           velocity ω_T;
6          if An ACK is received then
7              A neighbor is discovered;
8              Continue sending and listening for other
               neighbors;
9          else
10             i++;
11             Go to Step 3;
12         end
13     else
14         Keep listening for 2p rounds with angle
           velocity ω_R;
15         if A beacon signal then
16             Reply an ACK immediately;
17         else
18             i++;
19             Go to Step 3;
20         end
21     end
22 else
23     Terminate;
24 end
```

Algorithm 1 only focuses on neighbor discovery. Or, we can use neighbor discovery algorithm to schedule the transmission: *when* the *neighbor is discovered, the transmitter can send a data packet* as *needed*. The motivations of integrating neighbor discovery with transmission scheduling are: (i) after each node discovers its neighbors, a scheduling algorithm will be executed anyway for packet transmissions; (ii) the position and orientation of a node may vary over time, and thus it is beneficial to immediately transmit a backlogged data packet when the target neighbor is discovered.

The detailed algorithm that integrates neighbor discovery and transmission scheduling is presented in Algorithm 2. Once a neighbor is discovered, a data packet is transmitted between two nodes, assuming greedy sources (i.e., there is always data to be transmitted for any other node in the network). This approach is particularly useful when the network topology is dynamic (e.g., with mobility). We evaluate the throughput performance of the algorithm in Section 6.

Algorithm 2. Hunting-based directional neighbor discovery algorithm with transmission scheduling

Algorithm 2: Hunting-based Directional Neighbor Discovery Algorithm with Transmission Scheduling

Each node generates its pseudo-slot sequence S consisting of its ID (l_0 bits), $\lfloor \frac{l_0}{2} \rfloor + 1$ "0" bits, and $\lceil \frac{l_0}{2} \rceil$ "1" bits;
$i \leftarrow 0$;
if $i < L$ **then**
  if $S(i) = 1$ **then**
    Continuously sends a beacon signal and listens for ACK alternatively for $2q$ rounds with angle velocity ω_T;
    if *An ACK is received* **then**
      A neighbor is discovered;
      Send a data packet to the discovered neighbor;
      $i \leftarrow 0$;
      Go to Step 3;
    else
      $i++$;
      Go to Step 3;
    end
  else
    Keep listening for $2p$ rounds with angle velocity ω_R;
    if *A beacon signal is received* **then**
      Reply an ACK immediately;
      Receive the data packet;
      $i \leftarrow 0$;
      Go to Step 2;
    else
      $i++$;
      Go to Step 3;
    end
  end
else
  Reset $i \leftarrow 0$; Go to Step 2;
end

4.3. Worst-case neighbor discovery time

Theorem 3 shows that neighbor discovery can be finished in bounded time, i.e., L pseudo-slots, which is an upper bound on the neighbor discovery time. To further analyze the performance of the proposed scheme, we derive the time needed to discover *all* neighbors, termed *worst case discovery time*, which is denoted as N_B, in number of beacon signal times (i.e., τ_B), by considering all possible initial beam directions, sequences rotations, and sequence drifts. According to the procedure described in Algorithm 1, the worst case discovery time can be derived as

$$N_B = 2Lp\frac{2\pi}{\omega_R \tau_B} = \frac{32pqL\pi}{p\theta_T + q\theta_R - 2\pi}. \tag{11}$$

Theorem 4. *A lower bound for the worst case neighbor discovery time is $64\pi^2 L/(\theta_T\theta_R)$, in number of beacon signal times.*

Proof. Consider the worst case neighbor discovery time, which is N_B beacon times as given in (11). The partial derivatives of N_B with respect to p and q can be derived as follows.

$$\frac{\partial N_B}{\partial p} = \frac{32ql\pi(q\theta_R - 2\pi)}{(p\theta_T + q\theta_R - 2\pi)^2}$$

$$\frac{\partial N_B}{\partial q} = \frac{32pl\pi(p\theta_T - 2\pi)}{(p\theta_T + q\theta_R - 2\pi)^2}.$$

On one hand, the potential minimal value of N_B, denoted as N_B^*, is at $\{p_0 = 2\pi/\theta_T, q_0 = 2\pi/\theta_R\}$, with $N_B^* = (64\pi^2 L)/(\theta_T\theta_R)$. On the other hand, we have $\frac{\partial^2 N_B}{\partial^2 p}|_{p=p_0} > 0$ and the Hessian is greater than 0. Therefore, $N_B^* = (64\pi^2 L)/(\theta_T\theta_R)$ is a lower bound for the worst case neighbor discovery time. ∎

5. Neighbor discovery under sidelobe effect

In previous sections, we derive the conditions and algorithms for directional neighbor discovery with an ideal antenna model. To examine the proposed algorithms in a more general scenario, we next consider neighbor discovery with a more general antenna pattern, and examine the impact of sidelobes on the performance of neighbor discovery.

5.1. Antenna pattern and sidelobe effects

Consider a directional antenna pattern composed of a main lobe and $K-1$ sidelobes. The Main Lobe to SideLobe ratio (MLSL) is M. Without losing generality, we ignore the differences among the sidelobes and assume that all lobes have the same beamwidth θ. The model is illustrated in Fig. 8. Let φ be the pointing angle. The antenna gain is modeled as

$$g(\varphi) = \begin{cases} G(\theta), & \varphi < \frac{\theta}{2} \text{ or } \varphi > 2\pi - \frac{\theta}{2} \\ \frac{G(\theta)}{M}, & \frac{2k\pi}{K} - \frac{\theta}{2} < \varphi < \frac{2k\pi}{K} + \frac{\theta}{2}, \\ & k = 1, 2, \ldots, K-1 \\ 0, & \text{otherwise.} \end{cases} \tag{12}$$

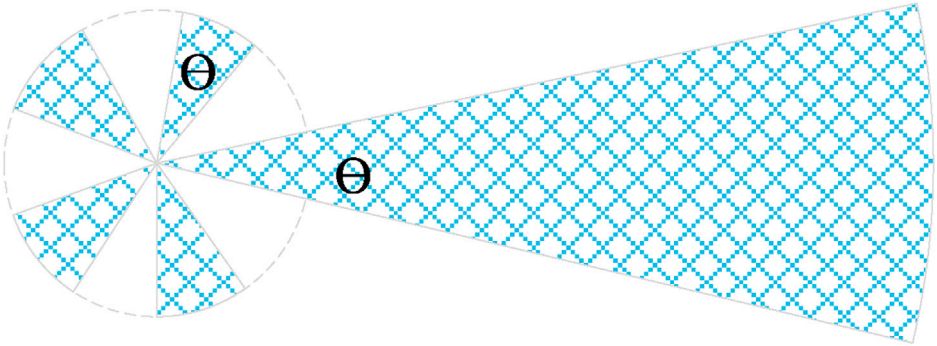

Fig. 8. The antenna model with sidelobes.

The main difference between the ideal single-beam antenna pattern and the antenna pattern with sidelobes is that a sidelobe can send or receive neighbor discovery beacon signals and ACK messages, which can increase the chance of neighbor discovery, as well as the chance of collision. It is thus interesting to examine how the sidelobe effect affects the neighbor discovery process. Taking into account the distance between any pair of nodes and the antenna model (12), there are the following four possible scenarios:

1. The two nodes cannot communicate with each other under any circumstances;
2. Only when two main lobes are used can they communicate with each other;
3. They can communicate with each other using one sidelobe and one main lobe;
4. They can communicate with each other using a pair of sidelobes.

The above four cases are ordered according to the corresponding communication ranges. The last three cases are related to neighbor discovery, while the latter two cases are relevant to the influence of sidelobes on neighbor discovery. Regarding the sidelobe effects on neighbor discovery, it is worth noting that if two nodes can communicate with sidelobes, they must be able to communicate with the main lobes as well. Therefore, the sidelobes do not help to discovery *more* neighbors; however, they can help to discover a neighbor *early*, thus reducing the neighbor discovery time. In Section 5.2, we analyze the portion of neighbors that can be discovered by sidelobes in an mmWave ad hoc network. In Section 5.3, we analyze the sidelobe effect on the worst-case neighbor discovery time.

5.2. Portion of neighbors discovered by sidelobes

In this section, we present a stochastic geometry [28]-based analysis to derive the portion of neighbors that can be discovered by sidelobes. It is assumed that the distribution of nodes follows the spatial Poisson Point Process (PPP) with density λ. Recall that a pair of nodes are considered as neighbors if they can complete a beacon signal/ACK handshake. Considering quasi-static channels, the transmission range of a link of both main lobes is r. Assuming a path loss exponent of 2 for the propagation model and following the antenna gain model (12), the range for a main lobe–sidelobe link is $r/\sqrt{M}$, and the range for a sidelobe–sidelobe link is r/M. Therefore, if two nodes are more than $r/\sqrt{M}$ apart, the sidelobes will have no impact on neighbor discover.

To evaluate the impact of sidelobe effect, we have the following definition for the portion of neighbors that can be discovered by sidelobes.

Definition 1. *For an arbitrary, tagged node, the number of its neighbors that can only communicate with main lobe–main lobe links is a random variable N_m; and the total number of its neighbors is another random variable N_a. Then, the* mainlobe coefficient *ε_m is defined as*

$$\varepsilon_m = \mathbb{E}\left[\frac{N_m}{N_a}\right]. \tag{13}$$

It is easy to see $0 \le \varepsilon_m \le 1$, while $1-\varepsilon_m$ is the portion of neighbors that can be detected by sidelobes. If all neighbors are $r/\sqrt{M}$ away from the tagged node, then we have $\varepsilon_m = 1$ and the sidelobes have no impact on neighbor discovery. Furthermore, the two random variables N_m and N_a are not independent. We have the following theorem for ε_m.

Theorem 5. *Considering the 2D spatial PPP network model with density λ, the transmission range for a pair of neighbors using their main lobes is r, and the MLSL is M. Then, the mainlobe coefficient can be derived as*

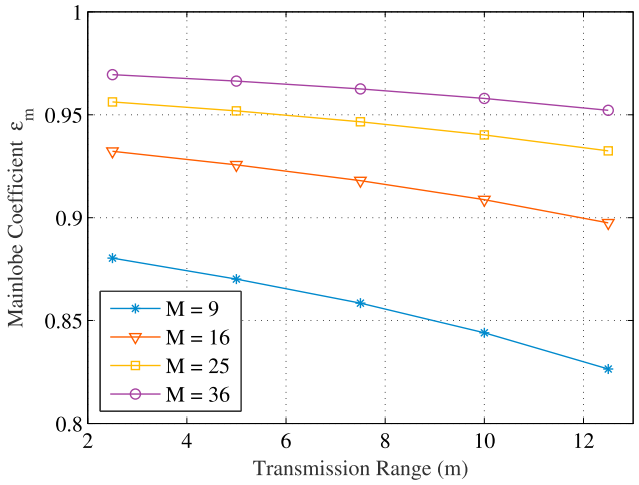

Fig. 9. The main lobe coefficient ε_m for different transmission ranges r with $\lambda = 0.25$.

$$\varepsilon_m = \sum_{0<z<1,\, z\in\mathbf{Q}} \sum_{v\in\mathbf{Z}^*} \frac{e^{-\lambda_1-\lambda_2}\lambda_1^{v-vz}\lambda_2^{vz}z}{\Gamma(v-vz+1)\Gamma(vz+1)}, \tag{14}$$

where $\lambda_1 = \lambda\pi r^2/M$, $\lambda_2 = \lambda\pi r^2(M-1)/M$, and $\Gamma(\cdot)$ is the gamma function.

Proof. The network is modeled as a PPP defined in the plane $\mathbf{R}^2$, for a fixed, bounded Borel measurable region $\mathbf{B}$ of the plane. Let the number of points falling in $\mathbf{B}$ be $N(\mathbf{B})$. Then, the probability of having n points in $\mathbf{B}$ is given by

$$\Pr(N(\mathbf{B}) = n) = \frac{(\lambda|\mathbf{B}|)^n}{n!}e^{-\lambda|\mathbf{B}|}, \tag{15}$$

where $|\mathbf{B}|$ denotes the area of region $\mathbf{B}$.

Consider the two neighborhoods (as Boral measurable regions) of the tagged node, with the radii r and $r/\sqrt{M}$, respectively. Define two random variables: X as the number of nodes within the radius $r/\sqrt{M}$ of the tagged node, and Y as the number of nodes outside the disk with radius $r/\sqrt{M}$ but inside radius r. Since the above two regions are disjoint, the distributions of X and Y are independent due to the property of PPP. Let $Z = Y/(X+Y)$, then we have

$$\varepsilon_m = \mathbb{E}\left[\frac{N_m}{N_a}\right] = \mathbb{E}\left[\frac{Y}{X+Y}\right] = \mathbb{E}[Z],$$

with

$$\Pr(X = x) = \frac{\left(\frac{\lambda\pi r^2}{M}\right)^x}{x!}\exp\left\{-\frac{\lambda\pi r^2}{M}\right\}$$

$$\Pr(Y = y) = \frac{\left(\frac{\lambda\pi r^2(M-1)}{M}\right)^y}{y!}\exp\left\{-\frac{\lambda\pi r^2(M-1)}{M}\right\}.$$

Define $V = X+Y$ and consider the joint distribution of Z and V, then we have $X = V(1-Z)$ and $Y = VZ$. It follows that

$$P_{Z,V}(z,v) = P_{X,Y}(v(1-z), vz),$$

$$0 < z < 1, z \in \mathbf{Q}, \text{ and } v \in \mathbf{Z}^*,$$

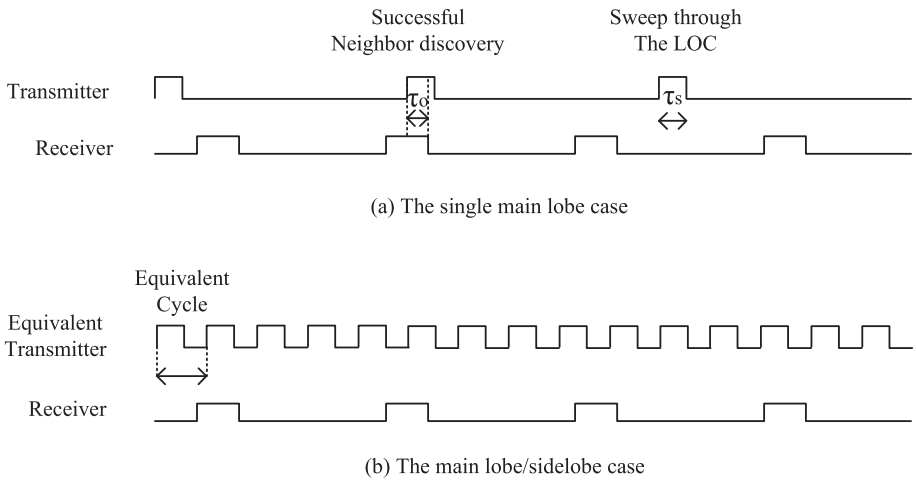

Fig. 10. Time line for nodes swap through the LOC of a pair of nodes during neighbor discovery process.

where $\mathbf{Q}$ is the set of rational numbers and $\mathbf{Z}^*$ is the set of non-negative integers. Thus, we have

$$\varepsilon_m = \mathbf{E}[Z] = \sum_{0<z<1,\, z\in\mathbf{Q}} \sum_{v\in\mathbf{Z}^*} \frac{e^{-\lambda_1-\lambda_2}\lambda_1^{v-vz}\lambda_2^{vz}z}{\Gamma(v-vz+1)\Gamma(vz+1)},$$

where $\lambda_1 = \lambda\pi r^2/M$ and $\lambda_2 = \lambda\pi r^2(M-1)/M$.

In Fig. 9, we plot the analytical results based on Theorem 5. The network area is 20×20 m^2, with $\lambda = 0.25/\text{m}^2$. For each fixed transmission range r, $r = 2.5, 5.0, 7.5, 10.0, 12.5$, we can see that ε_m increases as M gets larger. This is because M is increased, the sidelobe gain becomes smaller, and the sidelobe effect is weakened. To the extreme when M is ∞, it reduces to the single beam antenna model (1) and $\varepsilon_m = 1$. On the other hand, for each fixed M, $M = 9, 16, 25, 36$, ε_m decreases as the transmission range r is increased. This is because the area covered by the transmission range r is $A_1 = \pi r^2$, while the area covered by the ring between radius r and $A_2 = r\sqrt{M}$is $\pi r^2(M-1)/M$. As r is increased, the A_1 will increase faster than A_2.

5.3. Effect on the worst-case discovery time

From the above analysis, we find that the sidelobe effect will be limited when the antenna directivity is high or the network is sparse. However, sidelobes do affect the neighbor discovery process with respect to the worst-case neighbor discovery time. For the four scenarios shown in Section 5.1, in both scenarios 3 and 4, the sidelobes could help to find a near neighbor earlier. Reconsidering the conditions for successful neighbor discovery (see Section 3), now the transmitter and receiver can find each other if and only if their two beams (either the main lobe or sidelobe) sweep through the LOC with sufficient overlap time. For a near neighbor within the sidelobe range of the transmitter, both the main lobe and the sidelobes sweep through the LOC. Fig. 10(a) is the case for a main lobe–main lobe link; and Fig. 10(b) is an example for both main lobe-main lobe and main lobe–sidelobe links.

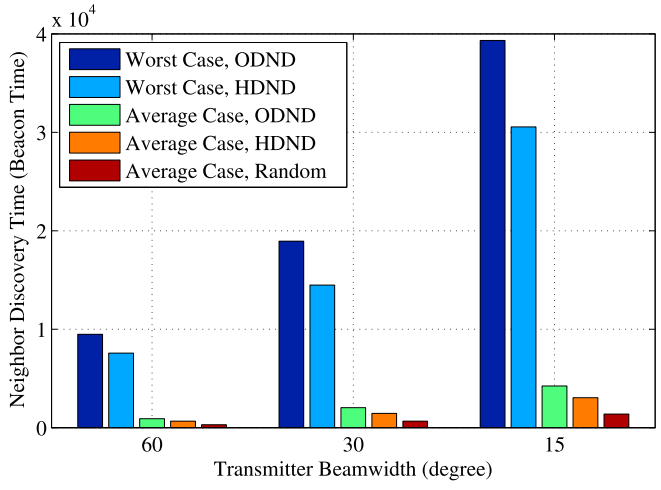

Fig. 11. Neighbor discovery time in the number of beacon signal times achieved by the three schemes when the receiver beamwidth $\theta_R = 72^\circ$.

As the proof of Theorem 1 shows, what really matters with respect to neighbor discovery is the time that the transmitter beam sweeps through the LOC connecting the transmitter and receiver, which is called *LOC time*. In the main lobe–main lobe case (see Fig. 10(a)), the LOC time is θ_T/ω_T within a period of $2\pi/\omega_T$. In the main lobe–main lobe and main lobe–sidelobe case (see Fig. 10(b)), the LOC time is $K\theta_T/\omega_T$ within a period of $2\pi/\omega_T$. The latter is equivalent to a new transmitter with the beam width $K\theta$ and the angular speed $K\omega$, which also has the LOC time of $K\theta_T/\omega_T$ within a period of $2\pi/\omega_T$. Following the above reasoning and (11), and considering the fact that $\omega_R/\omega_T = p/q$, we have the following result.

Theorem 6. *With the antenna pattern* (12)*, the worst-case neighbor discovery time is*

$$N_B = \begin{cases} \dfrac{32pqL\pi}{p\theta_T + q\theta_R - 2\pi}, & \text{for main lobe–main lob links} \\ \dfrac{32pqL\pi}{p\theta_T + q\theta_R - 2\pi/K}, & \text{for main lobe–sidelobe links} \\ \dfrac{32pqL\pi}{p\theta_T + q\theta_R - 2\pi/K^2}, & \text{for sidelobe–sidelobe links.} \end{cases} \quad (16)$$

Theorem 6 indicates that the sidelobes do reduce the worst-case neighbor discovery time if *all* nodes are within the sidelobe transmission range (lines 2 and 3 in (16)). If there are still some nodes that can only communicate with their main lobes, the worst-case neighbor discover time will still be determined by the first line in (16), which is the same as (11).

6. Simulation study

6.1. Simulation setting

In this section, we present our simulation study on validating the proposed Hunting-based Directional Neighbor Discovery (HDND) algo-

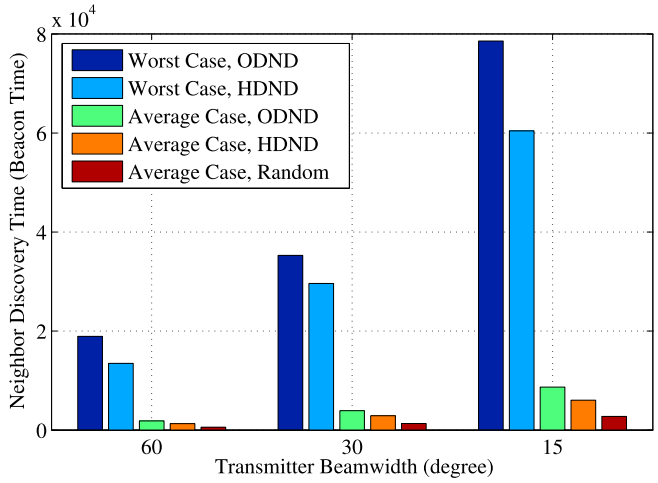

Fig. 12. Neighbor discovery time in the number of beacon signal times achieved by the three schemes when the receiver beamwidth $\theta_R = 360^\circ/11 = 32.73^\circ$.

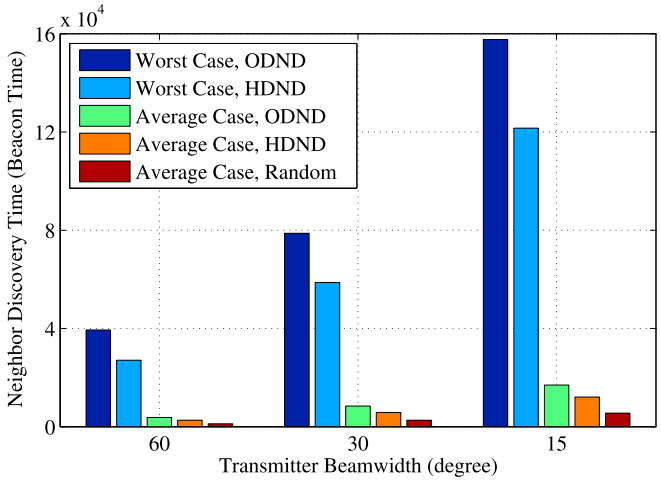

Fig. 13. Neighbor discovery time in the number of beacon signal times achieved by the three schemes when the receiver beamwidth $\theta_R = 360^\circ/23 = 15.65^\circ$.

rithm. We have implemented Algorithms 1 and 2 in Matlab and conducted extensive simulations. The simulations for the case of one pair of nodes are repeated 200,000 times with different random seeds, considering random initial delay, random drift between the two sequences, and random original beam orientations. The initial delay is uniformly distributed in $[0, 100{,}000]$ beacon signal times. We choose the beamwidth for the reception mode as 72°, $360^\circ/11 = 32.73^\circ$, and $360^\circ/23 = 15.65^\circ$, and the beamwidth for the transmission mode as 60°, 30°, and 15° as in Ref. [13]. The values of other parameters are varied during the simulations to investigate the performance of neighbor discovery.

The Oblivious Directional Neighbor Discovery (ODND) algorithm (ODND) proposed in Ref. [23] (where each node follows the directional sequence assigned according to the Chinese Remainder Theorem, such that any pair of nodes will face any combination of directions) and a *random scheme* (where each node randomly points its beam to arbitrary directions) are used as baselines and simulated under the same settings for comparison. In Section 6.5, we also use the Multi-Band Neighbor Discovery (MBND) scheme [15] as the baseline scheme for throughput comparisons, where all nodes are within a one-hop network on a 2.4 GHz WiFi channel and coordinated by the central controller for neighbor discovery and transmission scheduling.

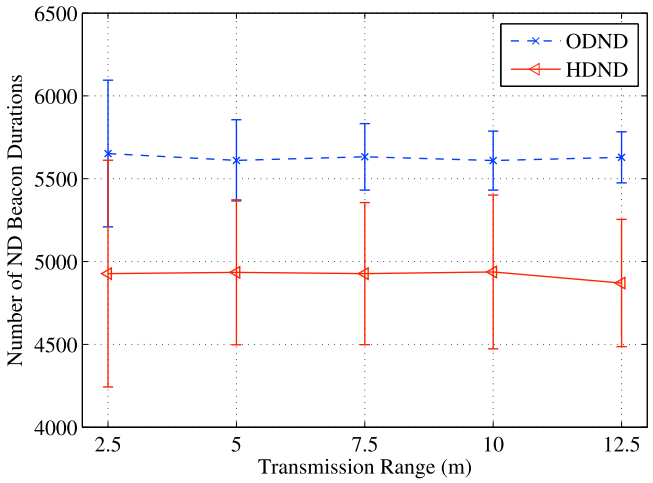

Fig. 14. Average case neighbor discovery time versus transmission range achieved by HDND and ODND.

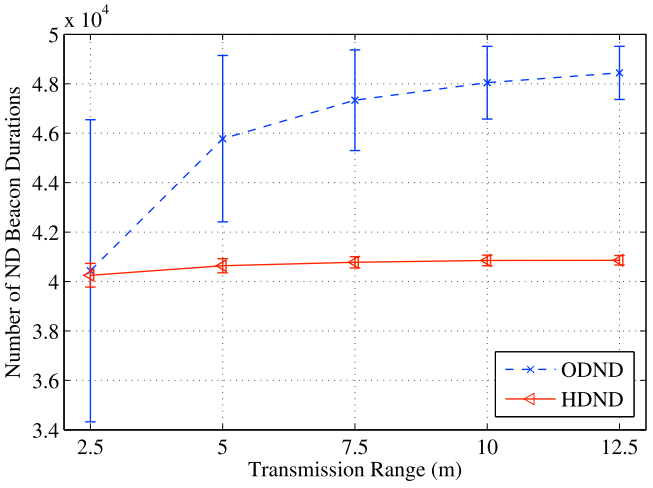

Fig. 15. Worst-case neighbor discovery time versus transmission range achieved by HDND and ODND.

6.2. *Neighbor discovery for a pair of nodes*

In Figs. 11–13, the neighbor discovery times for different parameter settings are presented. It can be seen that HDND outperforms ODND in all the cases on both worst-case discovery time and average case discovery time. For example, in Fig. 11, when the transmitter antenna beamwidth is 15°, the worst-case discovery time (in number of beacon signal times τ_B) of ODND is 39330, while the worst-case discovery time for HDND is 30547. HDND achieves a 22.3% reduction in the worse case discovery time over ODND. The average discovery time of ODND is 4288.6, while the average discovery time of HDND is 3034, which is a 29.3% reduction over ODND. Although the average discovery time of the Random scheme is the lowest, its worst-case discovery time is actually ∞ (i.e., in many cases it fails to discover the neighbor), while both HDND and ODND can guarantee successful neighbor discovery. The discovery times (worst-case and average case) of all the schemes increase as the antenna beamwidths are reduced, due to the more severe deafness effect caused by the increased directivity of the directional antennas.

To make a fair comparison with ODND, we relax the ideal beacon signal assumption made for ODND in Ref. [23], and use real beacon signals with a non-zero transmission time in the simulations. We set 10 beacon signal times per slot since the positions of beacon signals in

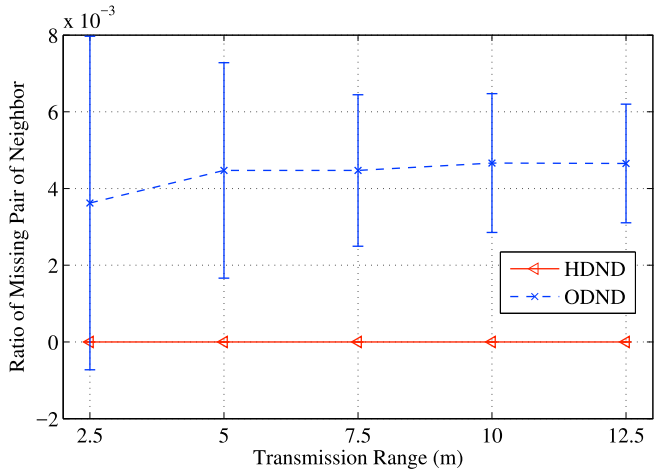

Fig. 16. Error detection rate versus transmission range achieved by HDND and ODND.

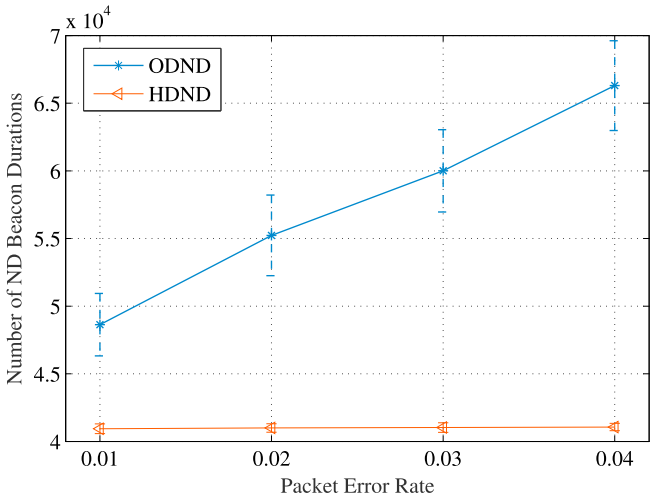

Fig. 18. Worst-case neighbor discovery time under transmission errors achieved by HDND and ODND.

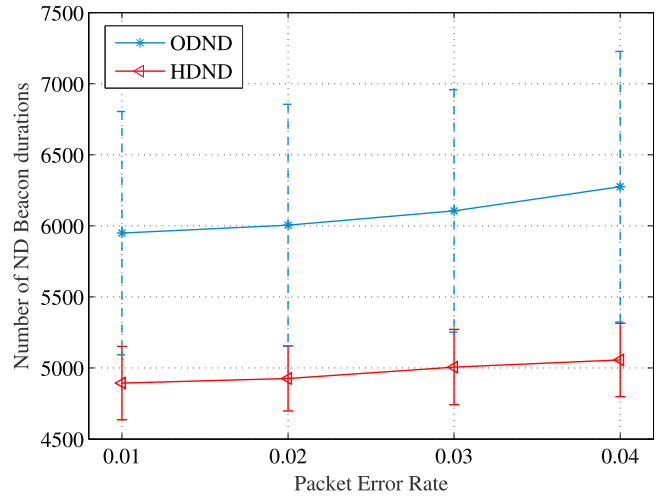

Fig. 17. Average case neighbor discovery time under transmission errors achieved by HDND and ODND.

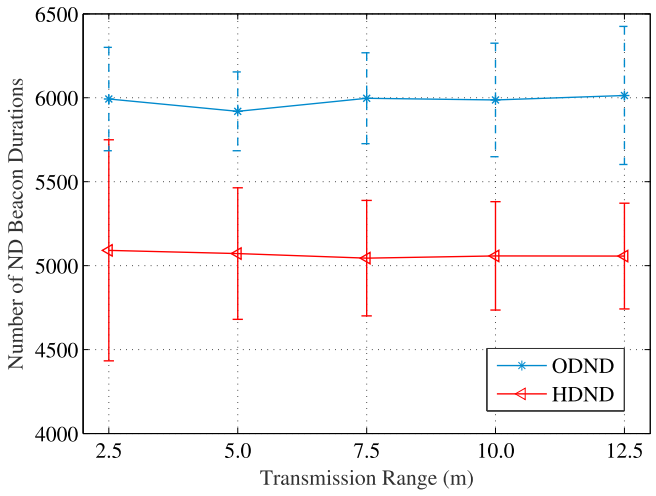

Fig. 19. Average case neighbor discovery time under the sidelobe effect for HDND and ODND.

Ref. [23] are at the 10% and 20% positions in a slot. Otherwise, there will be a collision even without considering the drift effect. For the Random scheme, a pair of nodes may not discover each other within 200,000 beacon signal times. The simulations also show that ODND may not always discover all neighbors when the ideal beacon signal assumption is removed. From Figs. 11–13, we find the proposed HDND algorithm is about 1.3–1.5 times faster than the ODND scheme in both worst-case delay and average delay in all the simulated scenarios.

6.3. Neighbor discovery in ad hoc networks

We next examine neighbor discovery in a distributed mmWave ad hoc network, and the results are presented in Figs. 14–16. In these simulations, 100 nodes are randomly placed in a square area of 20.0× 20.0 m^2. The simulation parameters are summarized in Table 1. The unit time is still the beacon signal time τ_B. For example, in Fig. 14, a value of 5,000 indicates 5,000τ_B s. The network topology is randomly generated for each simulation configuration. The error bars are 95% confidence intervals. From Figs. 14 and 15, it can be seen that HDND's average and worst-case total neighbor discovery times are both almost constant as the transmission range increases from 2.5 m to 12.5 m. ODND's average discovery time also remains constant for different transmission ranges, but its worst-case discovery time increases with the increase of transmissions range. Still, HDND is about 1.4 times faster than ODND in terms of average neighbor discovery time in all the cases.

The error detection ratios achieved by HDND and ODND are presented in Fig. 16 for the mmWave ad hoc network simulations following the setting in Ref. [23]. As Fig. 16 shows, the error detection rate of HDND is almost 0% for all simulated cases, i.e., it can find almost all the neighbors. In contrast, ODND has a 0.4% chance to miss neighbors due to collision of beacon signals. Note that the missed detection of neighbors in HDND is caused by collisions of beacon signals only. If the same ideal beacon assumption is made (i.e., extremely short beacon signals with a zero transmission time), the missed detection rate of HDND will be zero.

To evaluate the proposed HDND scheme in more realistic scenarios, we next investigate the impact of transmission errors (i.e., loss of beacon signals or ACKs due to transmission errors). Clearly, the loss of beacon signals and/or ACKs will reduce the success rate of neighbor discovery or increase the time of neighbor discovery. The impact of errors can be mitigated by adopting a stronger error correction code for beacon signals and ACKs. We simulate beacon/ack transmissions with different packet error rates. The results are shown in Figs. 17 and 18. Not surprisingly, for both the benchmark scheme and the proposed scheme, the average and worst neighbor discovery time both increase as the packet error rate

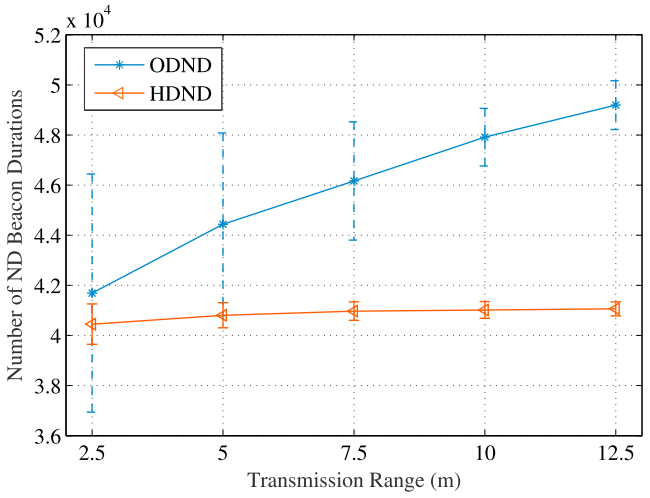

Fig. 20. Worst case neighbor discovery time under the sidelobe effect for HDND and ODND.

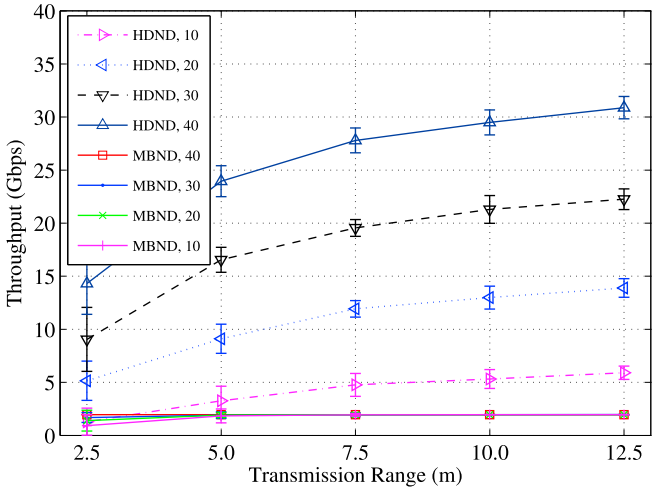

Fig. 21. Network-wide throughput under different transmission ranges.

increases. However, it can be seen that the proposed scheme still outperforms the benchmark scheme with considerable gains. The worst-case neighbor discovery time of HDND is rather robust to transmission errors. When the packet error rate is increased from 0.01 to 0.04, the worst -case neighbor discovery time of HDND only slightly increases from 40940 to 41063, while the worst-case neighbor discovery time of ODND increases from 48632 to 66298.

6.4. Sidelobe effect

We also consider the impact of sidelobes. The antenna pattern for this simulation consists of a main lobe with a beamwidth of 30°, as well as 8 sidelobes on the remaining directions, each with a beamwidth of 15°. The gain of each sidelobe is 6.73 dB down from that of the main lobe. Similar to the main lobe, a sidelobe can also send or receive beacon signals and cause interference/collisions to other signals when and only when the sidelobe overlaps with other beams [2]. The simulation results are presented in Figs. 19 and 20.

From Figs. 19 and 20, it can be seen that the average neighbor discovery time does not change much with the sidelobe effect since the sidelobe effect is dependent on the distance between the neighbors. If two nodes are in the transmission range such that they can communicate with each other only with their main lobes, the sidelobes do not affect the neighbor discovery performance at all. If two nodes are close enough, the sidelobe effect will bring more opportunities of neighbor discovery, as well as more collisions. Thus, the sidelobe effect causes more uncertainty, especially when the network is dense. This can be seen in Fig. 20; the worst-case neighbor discovery time of HDND increases slightly compared to that in Fig. 15 due to the uncertainty caused by the sidelobes.

6.5. Throughput performance

Finally, we evaluate the performance of Algorithm 2 that conducts joint neighbor discovery and transmission scheduling. Since HDND achieves a more significant reduction in neighbor discovery time than ODND, as shown in Figs. 11–20, this would directly translate into a high throughput gain in a real-world network. In addition, ODND does not include a transmission scheduling component. Therefore, we consider the Multi-Band Neighbor Discovery (MBND) scheme [15] as a baseline scheme for comparison.[3] With MBND, the nodes are scheduled to conduct directional neighbor discovery in the mmWave band, one node pair at a time. The simulation parameters are listed in Table 1. Each simulation is repeated 30 times, each time with a randomly generated topology. The 95% confidence intervals are computed and plotted in the figures as error bars. We consider greedy source, where each node always has a full buffer of data to send to each neighbor.

The throughput results are presented in Fig. 21 for increased transmission range. The values of p and q are set according to Theorems 1 and 2, as $p = 13$ and $q = 12$. We find that the throughput of Algorithm 2 increases as the number of nodes in the network increases, as well as the transmission range increases. In contrast, the MBND curves only increase slightly with the increase of network density and transmission range. The results show that with the proposed scheme in Algorithm 2, the network capacity can be enhanced when more neighbors are discovered, by allowing more concurrent transmissions. The MBND throughput performance is limited by the CSMA/CA mechanism on the 2.4 GHz WiFi control channel, which usually becomes the bottleneck of the system. There are significant gains on throughput achieved by the proposed Algorithm 2 over MBND, and the gain is greater for larger networks and longer transmission ranges. For example, when the transmission range is 2.5 m and there are 40 nodes in the network, the Algorithm 2 throughput is 14.31 Gbps and the MBND throughput is 1.96 Gbps, which is a 7.3 times gain. When the transmission range is 12.5 m for the same network, the Algorithm 2 throughput is 30.89 Gbps and the MBND throughput is 1.9614 Gbps, a 15.75 times gain.

7. Conclusions

In this paper, we developed an HDND scheme for mmWave ad hoc networks, where nodes rotate their antenna beams to search for neighbors. Based on a rigorous analysis, we derived the conditions for guaranteed neighbor discovery as well as a bound for the worst-case discovery time. The proposed HDND scheme does not require any control channels, nor any omni-directional transmissions, synchronized operation or time synchronization. Its performance was validated with extensive simulations. The results demonstrate remarkable improvement in neighbor discovery time, and striking increases in throughput over a wide range of network topologies compared to prior work.

[3] We chose MBND as a benchmark since it is a recent related work on the topic. Note that the comparison may not be a perfect one, since the design, requirements, and architecture of these two schemes are quite different. Unlike HDND, MBND uses 2.4 GHz WiFi for neighbor discovery and thus the throughput of MBND can be low if the discovery time is considered. However, MBND can provide low discovery time even in mobile and dense environments since the discovery procedure can be completed in one shot.

Declaration of competing interest

I am an associate editor of DCN. I have no COI with the lead GE.

Acknowledgments

This work was supported in part by the NSF under Grants ECCS-1923717 and CNS-1320472, and by the Wireless Engineering Research and Education Center, Auburn University, Auburn, AL, USA.

References

[1] Y. Wang, S. Mao, T.S. Rappaport, On directional neighbor discovery in mmWave networks, in: Proc. IEEE ICDCS 2017, June 2017, pp. 1–10. Atlanta, GA.
[2] T.S. Rappaport, R.W. Heath, R.C. Daniels, J.N. Murdock, Millimeter Wave Wireless Communications, Prentice Hall, Upper Saddle River, NJ, 2014.
[3] T.S. Rappaport, S. Sun, R. Mayzus, H. Zhao, Y. Azar, K. Wang, F. Gutierrez, Millimeter wave mobile communications for 5G cellular: it will work!, IEEE Access J. 1 (May 2013) 335–349.
[4] Z. He, S. Mao, "Adaptive multiple description coding and transmission of uncompressed video over 60GHz networks, ACM Mobile Comput. Commun. Rev. 18 (1) (Jan. 2014) 14–24.
[5] S. Sun, T.S. Rappaport, T.A. Thomas, A. Ghosh, H.C. Nguyen, I.Z. Kovacs, I. Rodriguez, O. Koymen, A. Partyka, Investigation of prediction accuracy, sensitivity, and parameter stability of large-scale propagation path loss models for 5G wireless communications, IEEE Trans. Veh. Technol. 65 (5) (May 2016) 2843–2860.
[6] H.N. Dai, K.W. Ng, M. Li, M.Y. Wu, An overview of using directional antennas in wireless networks, Int. J. Commun. Syst. 26 (4) (Apr. 2013) 413–448.
[7] T. Ohira, K. Gyoda, Electronically steerable passive array radiator antennas for low-cost analog adaptive beamforming, in: Proc. IEEE Phased Array 2000, May 2000, pp. 101–104. Dana Point, CA.
[8] Z. He, S. Mao, T.S. Rappaport, On link scheduling under blockage and interference in 60 GHz ad hoc networks, IEEE Access J. 3 (Sept. 2015) 1437–1449.
[9] Z. He, S. Mao, A decomposition principle for link and relay selection in dual-hop 60 GHz networks, in: Proc. IEEE INFOCOM 2016, Apr. 2016, pp. 1683–1691. San Francisco, CA.
[10] I.K. Son, S. Mao, M.X. Gong, Y. Li, On frame-based scheduling for directional mmWave WPANs, in: Proc. IEEE INFOCOM 2012, Mar. 2012, pp. 2149–2157. Orlando, FL.
[11] I.-K. Son, S. Mao, Y. Li, M. Chen, M.X. Gong, T.S. Rappaport, Frame-based medium access control for 5G wireless networks, Springer MONET Journal 20 (6) (Dec. 2015) 763–772.
[12] R. Ramanathan, J. Redi, C. Santivanez, D. Wiggins, S. Polit, Ad hoc networking with directional antennas: a complete system solution, IEEE Sel. Areas Commun. 23 (3) (Mar. 2005) 496–506.
[13] S. Vasudevan, J. Kurose, D. Towsley, On neighbor discovery in wireless networks with directional antennas, in: Proc. IEEE INFOCOM'05, Mar. 2005, pp. 2502–2512. Miami, FL.
[14] M.X. Gong, R.J. Stacey, D. Akhmetov, S. Mao, A directional CSMA/CA protocol for mmWave wireless PANs, in: Proc. IEEE WCNC 2010, Apr. 2010, pp. 1–6. Sydney, Australia.
[15] H. Park, Y. Kim, T. Song, S. Pack, Multiband directional neighbor discovery in self-organized mmWave ad hoc networks, IEEE Trans. Veh. Technol. 64 (3) (Mar. 2015) 1143–1155.
[16] J. Ning, T.S. Kim, S.V. Krishnamurthy, C. Cordeiro, Directional neighbor discovery in 60 GHz indoor wireless networks, Perform. Eval 68 (9) (Sept. 2011) 897–915.
[17] S. Sun, T.S. Rappaport, Millimeter wave MIMO channel estimation based on adaptive compressed sensing, in: Proc. IEEE ICC 2017-Workshops, May 2017, pp. 47–53. Paris, France.
[18] P.A. Eliasi, S. Rangan, T.S. Rappaport, Low-rank spatial channel estimation for millimeter wave cellular systems, IEEE Trans. Wireless Commun. 16 (5) (May 2017) 2748–2759.
[19] C.N. Barati, S.A. Hosseini, S. Rangan, P. Liu, T. Korakis, S.S. Panwar, T.S. Rappaport, Directional cell discovery in millimeter wave cellular networks, IEEE Trans. Wireless Commun. 14 (12) (Dec. 2015) 6664–6678.
[20] C.N. Barati, S.A. Hosseini, M. Mezzavilla, T. Korakis, S.S. Panwar, S. Rangan, M. Zorzi, Initial access in millimeter wave cellular systems, IEEE Trans. Wireless Commun. 15 (12) (Sept. 2016) 7926–7940.
[21] W.B. Abbas, M. Zorzi, Context information based initial cell search for millimeter wave 5G cellular networks, in: IEEE EuCNC 2016, June 2016, pp. 111–116. Athens, Greece.
[22] Y. Li, J.G. Andrews, F. Baccelli, T.D. Novlan, J.C. Zhang, Design and analysis of initial access in millimeter wave cellular networks, IEEE Trans. Wireless Commun. 16 (10) (Oct. 2017) 6409–6425.
[23] L. Chen, Y. Li, A.V. Vasilakos, Oblivious neighbor discovery for wireless devices with directional antennas, in: Proc. IEEE INFOCOM 2016, Apr. 2016, pp. 1–9. San Francisco, CA.
[24] M.K. Samimi, T.S. Rappaport, 3-D millimeter-wave statistical channel model for 5G wireless system design, IEEE Trans. Microw. Theory Techn. 64 (7) (July 2016) 2207–2225.
[25] K. Ireland, M. Rosen, A Classical Introduction to Modern Number Theory, second ed., Springer-Verlag, Berlin, Germany, 1990.
[26] L. Chen, K. Bian, Neighbor Discovery in Mobile Sensing Applications: A Comprehensive Survey, vol. 48, *Elsevier Ad Hoc Netw.*, Sept. 2016, pp. 38–52, vol. 1.
[27] K. Bian, J.-M. Park, Maximizing rendezvous diversity in rendezvous protocols for decentralized cognitive radio networks, IEEE Trans. Mobile Comput. 12 (7) (July 2013) 1294–1307.
[28] F. Baccelli, B. Błaszczyszyn, Stochastic geometry and wireless networks, volume I – theory, in: Foundations and Trends in Networking, vol. 3, NOW Publishers, 3/4, Delft, The Netherlands, 2009.
[29] T. Nitsche, C. Cordeiro, A.B. Flores, E.W. Knightly, E. Perahia, J.C. Widmer, IEEE 802.11 ad: directional 60 GHz communication for multi-Gigabit-per-second Wi-Fi, IEEE Commun 52 (12) (Dec. 2014) 132–141.
[30] R. Mudumbai, S. Singh, U. Madhow, Medium access control for 60 GHz outdoor mesh networks with highly directional links, in: Proc. IEEE INFOCOM 2009, Apr. 2009, pp. 2871–2875. Rio de Janeiro, Brazil.
[31] X. An, R.V. Prasad, I. Niemegeers, Neighbor discovery in 60 GHz wireless personal area networks, in: Proc. IEEE WoWMoM 2010, Canada, Montreal, June 2010, pp. 1–8.
[32] Y. Qiu, S. Li, X. Xu, Z. Li, Talk More Listen Less: energy-efficient neighbor discovery in wireless sensor networks, in: Proc. IEEE INFOCOM 2016, Apr, San Francisco, CA, 2016, pp. 1–9.
[33] Z. Zhang, DTRA: directional transmission and reception algorithms in WLANs with directional antennas for QoS support, IEEE Netw. 19 (3) (May/June 2005) 27–32.
[34] E. Felemban, R. Murawski, E. Ekici, S. Park, K. Lee, J. Park, Z. Hameed, SAND: Sectored-antenna neighbor discovery protocol for wireless networks, in: Proc. IEEE SECON 2010, June 2010, pp. 1–9. Boston, MA.
[35] B. Liu, B. Rong, R. Hu, Y. Qian, Neighbor discovery algorithms in directional antenna based synchronous and asynchronous wireless ad hoc networks, IEEE Wireless Commun 20 (6) (Dec. 2013) 106–112.
[36] R.B. Ertrel, P. Cardieri, K.W. Sowerby, T.S. Rappaport, J.H. Reed, Overview of spatial channel models for antenna array communication systems, IEEE Personal Commun (Feb. 1998) 10–22.